

# Supplementary Information (SI)

## Handheld and integrated single-cell pipettes

Kai Zhang,<sup>†,‡</sup> Xin Han,<sup>†,‡</sup> Ying Li,<sup>†,‡</sup> Sharon Yalan Li,<sup>†</sup> Youli Zu,<sup>§</sup> Zhiqiang Wang,<sup>¶</sup> Lidong Qin<sup>\*,†,‡,§</sup>

<sup>†</sup>Department of Nanomedicine, Houston Methodist Research Institute, Houston, TX 77030, USA

<sup>‡</sup>Department of Cell and Developmental Biology, Weill Medical College of Cornell University, New York, NY 10065, USA

<sup>§</sup>Department of Pathology and Genomic Medicine, Houston Methodist Hospital, Houston, TX 77030, USA

<sup>¶</sup>Department of Chemistry, Tsinghua University, Beijing 100084, China

<sup>§</sup>Department of Molecular and Cellular Oncology, The University of Texas M. D. Anderson Cancer Center, Houston, TX 77030, USA

\*Corresponding Author: [lqin@houstonmethodist.org](mailto:lqin@houstonmethodist.org)

## **Materials and methods**

### **Design and fabrication of the hSCP and iSCP tips.**

All designs were drawn with AutoCAD software (Autodesk) and printed out as glass photomasks (Photo Sciences, Inc.). The hSCP tip was fabricated by standard photolithography and elastomer molding. Briefly, SU-8 3025 negative photoresist (MicroChem Corp.) was used to fabricate a 17- $\mu\text{m}$  thick microstructure. Polydimethylsiloxane (PDMS; 10A:1B; Dow Corning Corp.) was poured onto the photoresist mold and heated at 80°C for 25 min. After curing, the PDMS was peeled off, and holes were drilled. Then, the PDMS layer (3-mm thickness) containing the microstructure was irreversibly bonded with an intact PDMS layer (0.5-mm thickness) using plasma treatment (Plasma ETCH, INC) to form an enclosed chip. The chip was left at 80°C for 1 h to enhance the bonding. Finally, the chip was cut to the appropriate size and shape using a scalpel to form the hSCP tip. Bonding is not required for iSCP tips fabrication. The round PDMS slab can be placed onto a standard Petri dish without thermal or oxygen-plasma treatment.

### **Preparation of cell cultures and cell suspensions.**

The SK-BR-3 (ATCC), MDA-MB-231/GFP (Cell Biolabs), and SUM 159 (Asterand) cell lines were cultured in Dulbecco's modified Eagle medium (DMEM) supplemented with 10% (v/v) fetal bovine serum (FBS) and 1% penicillin-streptomycin. All cells were grown in a humidified atmosphere of 5% (v/v) CO<sub>2</sub> at 37°C. Adherent cells on a 75 cm<sup>2</sup> flask were harvested by trypsin digestion and dispensed into a cell suspension at a concentration of 10<sup>6</sup>–10<sup>7</sup> cells/mL.

### **Detailed operation of single-adherent cell isolation.**

The PDMS slab of iSCP tips was laid onto a 50-mm diameter Petri dish without thermal or oxygen plasma treatment. Isolation of single adherent cells was achieved in four steps: capture, washing, culture, and release and transfer. (1) Capture. Cell suspensions (20  $\mu\text{L}$ ) with concentrations of 10<sup>6</sup>–10<sup>7</sup> cells/mL were added into the inlet of cell suspensions. A 1-mL capacity plastic syringe was used to slightly press the inlet and then gentle positive pressure was applied for 10 seconds to load suspended cells into the microchannels. During this procedure, single cells could be efficiently captured by single hooks. (2) Washing. Cells in the inlet were completely replaced by cell-free medium. Then gentle positive pressure was applied to the inlet for 10 seconds using a syringe in order to wash out all of the un-captured cells. (3) Culture. Placement of the iSCP tips into a standard cell incubator allows the isolated single cells to adhere, spread, and proliferate within the iSCP tips. (4) Release and transfer. After identification and selection of single adherent cells with the desired morphological phenotype, such as cell membrane protrusion, trypsin solution was slowly loaded into the port connected to the bypass microchannel by syringe. The single adherent cells were released from the hooks, and flowed into the cell outlet and were finally transferred into a designated container by hADP.

**Theoretical calculation of fluid resistance.**

The fluid resistance the along capture path ( $R_c$ ) and bypass path ( $R_b$ ) was estimated according to the previously described method<sup>1</sup>.

**Single-cell droplet volume evaluation.**

Single-cell droplet was transferred onto Petri dish surface and then rapidly weighed by a precise electronic balance (XS105 dual range analytical balances, Mettler Toledo).

**Single-cell PCR analysis.**

The single-cell PCR experiment (GenomePlex Single Cell Whole Genome Amplification Kit, Sigma-Aldrich) was implemented according to the manufacturer's instructions.

**Image acquisition and analysis.**

Bright-field, phase-contrast, and fluorescence images were obtained with an AMG EVOS fl digital inverted fluorescence microscope, an Olympus IX81 inverted fluorescence microscope, and a T3i Canon camera. Movies were filmed with the Olympus IX81 microscope and the T3i Canon camera.

**Reference**

1. Zhang, K., Chou, C.K., Xia, X., Hung, M.C. & Qin, L. *Proc. Natl. Acad. Sci. USA* **2014**, 111, 2948.

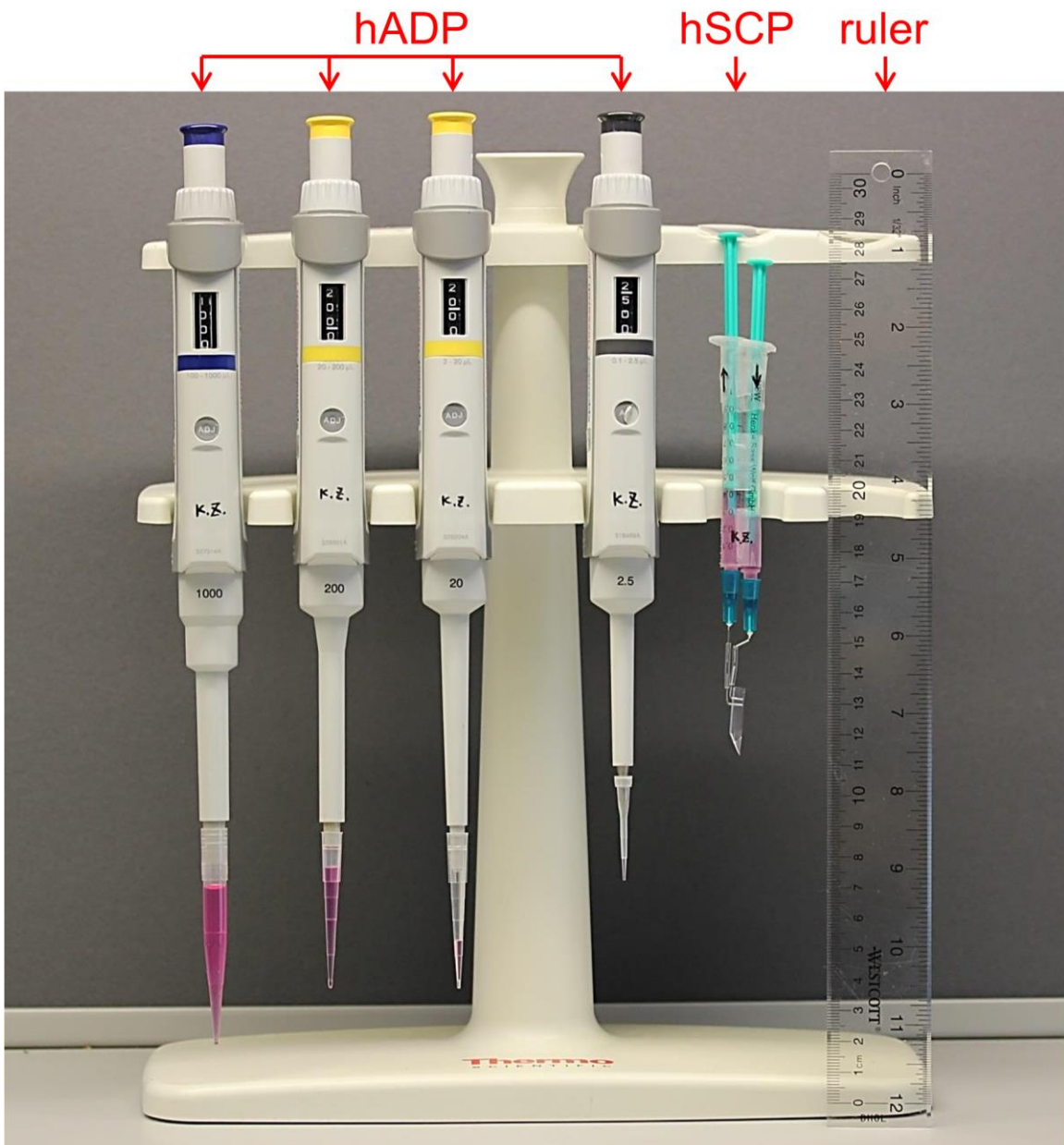


**Figure S1.** Image of four commercial hADPs and a proof-of-concept hSCP. Cell medium (red color) was aspirated into all tips. A ruler is included to indicate the dimensions.

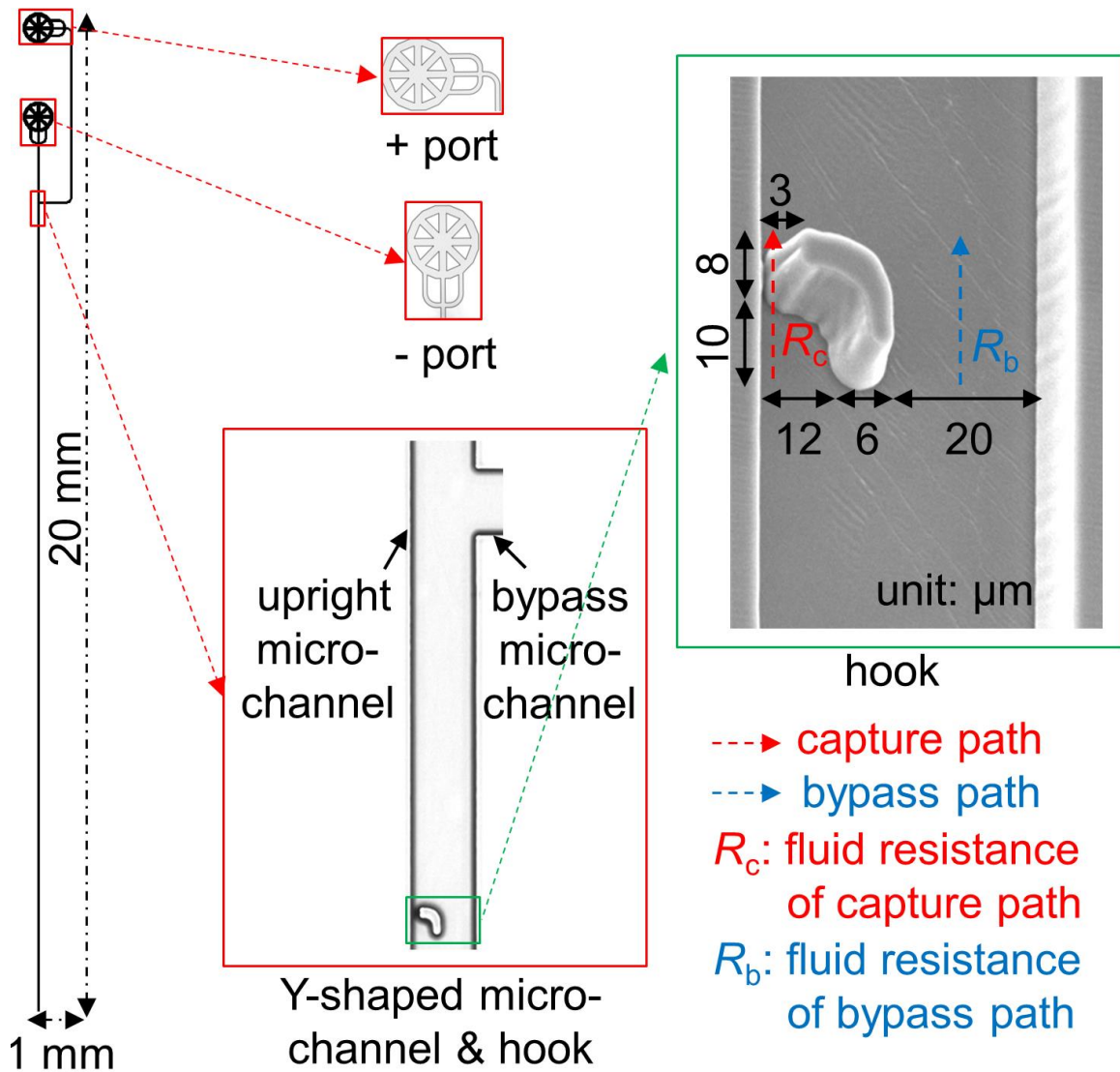


**Figure S2.** Design of hSCP tip. AutoCAD design of the hSCP tip with 20-mm length and 1-mm width. Microscopic images of a positive-pressure (+P) port, a negative-pressure (-P) port, upright and bypass microchannels, and a cell-capture hook are shown within three red rectangles, respectively. The magnified hook (scanning electron microscope) with detailed dimensions is presented within a green rectangle.  $R_c$  and  $R_b$  indicate fluid resistance of the capture path (red line) and the bypass path (blue line), respectively.

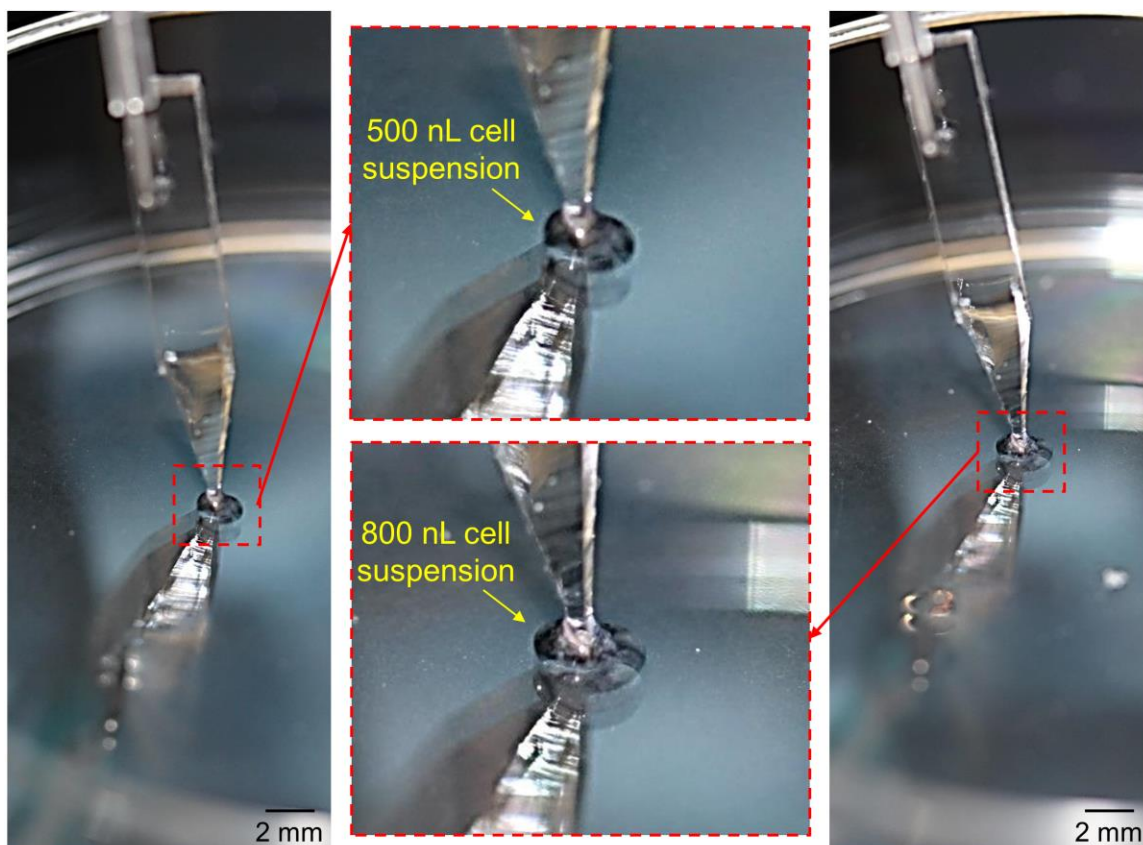


**Figure S3.** Images of hSCP for sampling directly from 500-nL and 800-nL cell suspensions placed on Petri dish surface.

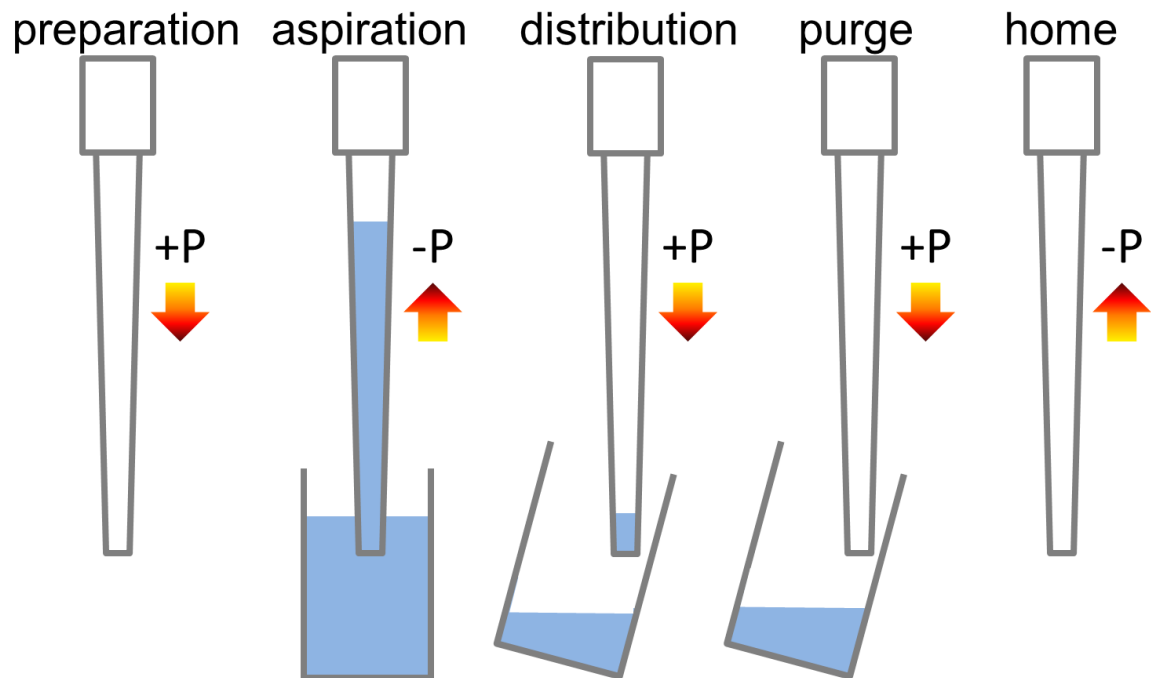


**Figure S4.** Work flow of handheld air-displacement pipette (hADP) for liquid distribution.

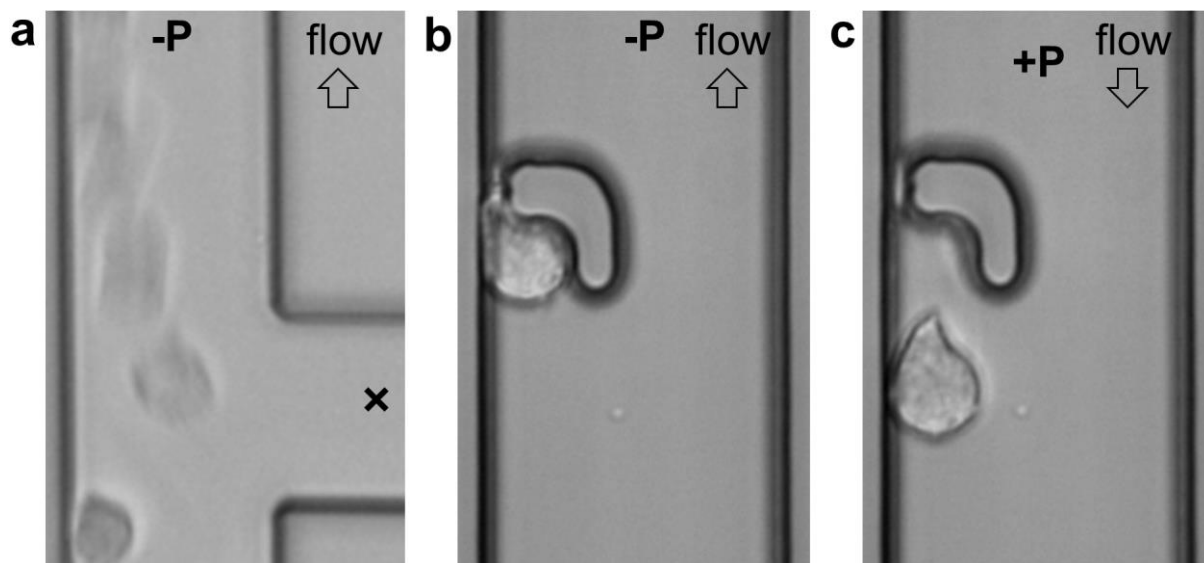


**Figure S5.** Snapshots of a cell moving along the upright microchannel (a), a captured single cell (b), and the captured single cell being released from the hook (c).

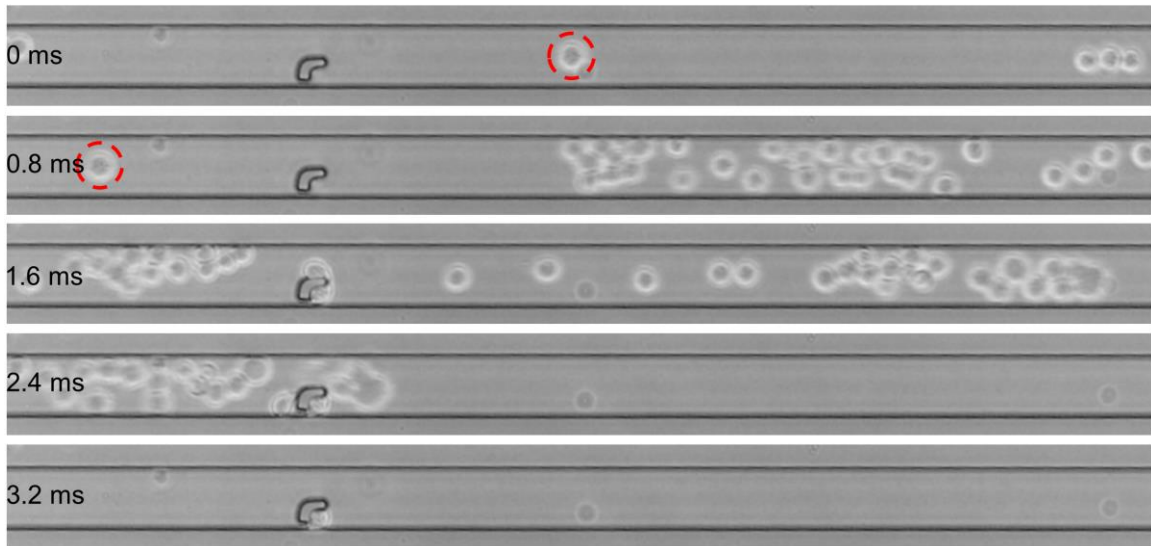


**Figure S6.** Sequential images of single-cell capture according to the cell-blocking effect. Due to the large fluid resistance of the capture path compared to the small resistance of the bypass path, cells (indicated by red dotted circle) preferentially flow along the center line of the bypass path and are not captured; however, successful single-cell capture frequently occurs when many cells pass the hook simultaneously. During this process, the bypass path is blocked by other cells and one cell is forced to flow along the capture path, and is captured by the hook. Time intervals are marked on the left of each image. SK-BR-3 cells were used.

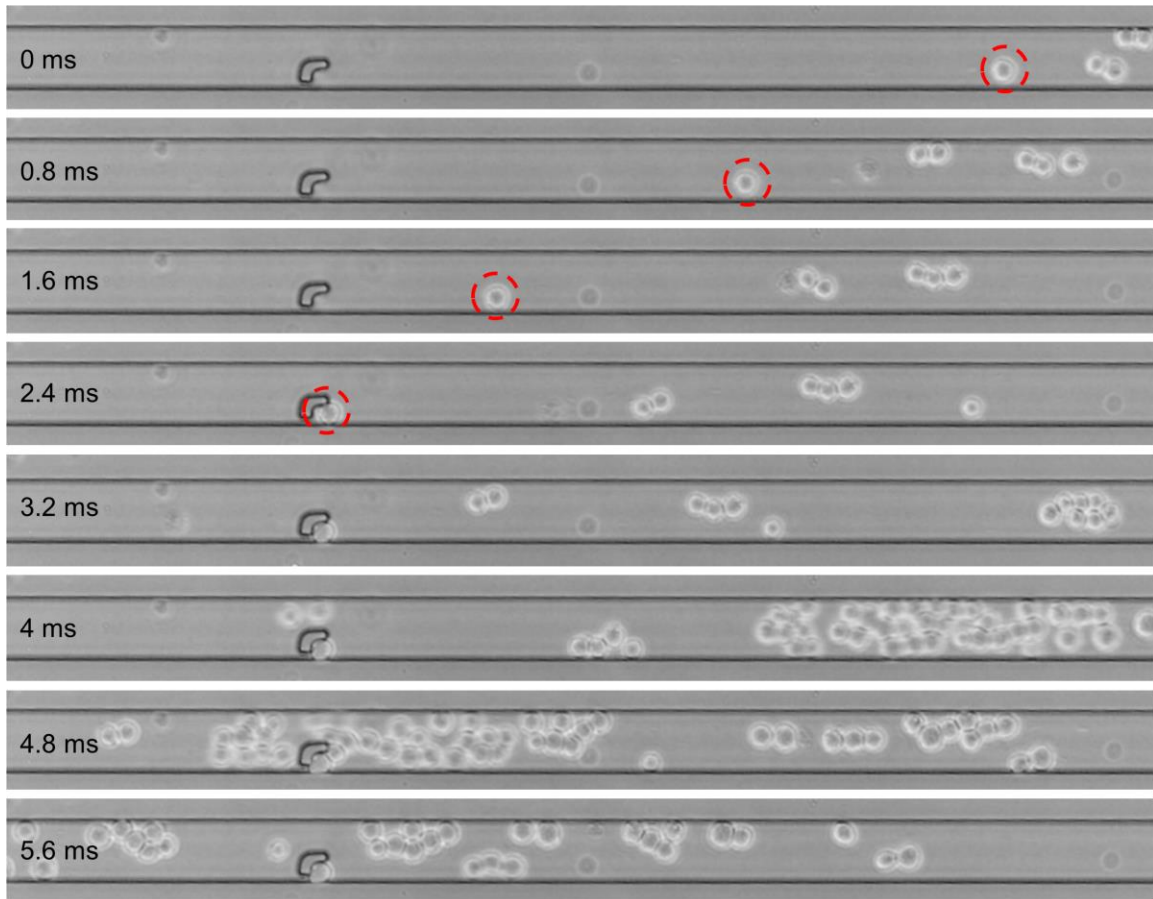


**Figure S7.** Sequential images of single-cell capture according to the laminar-flow effect. Due to the laminar-flow effect, a single cell (indicated by red dotted circles) occasionally flows along the wall of the upright microchannel and does not change its initial direction until capture by the hook. The captured single cell is very stable, and is not affected by subsequent large cell clusters. Time intervals are marked on the left of each image. SK-BR-3 cells were used.

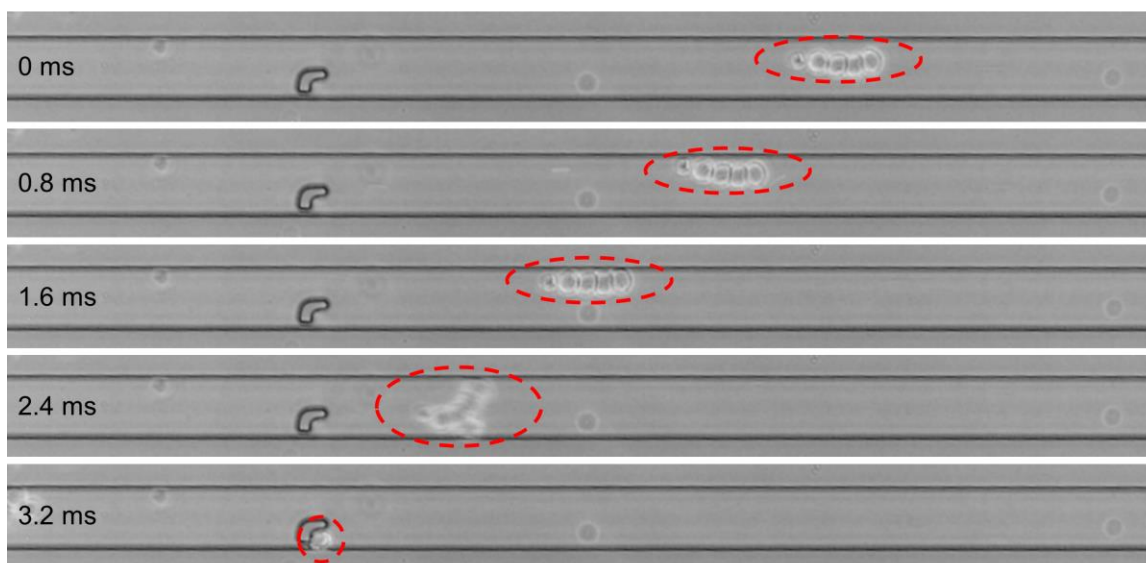


**Figure S8.** Sequential images of single-cell capture according to the temporary blocking effect. When approaching the hook, a cluster of cells (indicated by red dotted circles) changes its conformation due to changes in the flow profile in the upright microchannel. The new cell-cluster conformation temporarily blocks the bypass path, facilitating single-cell capture by the hook. Time intervals are marked on the left of each image. SK-BR-3 cells were used.

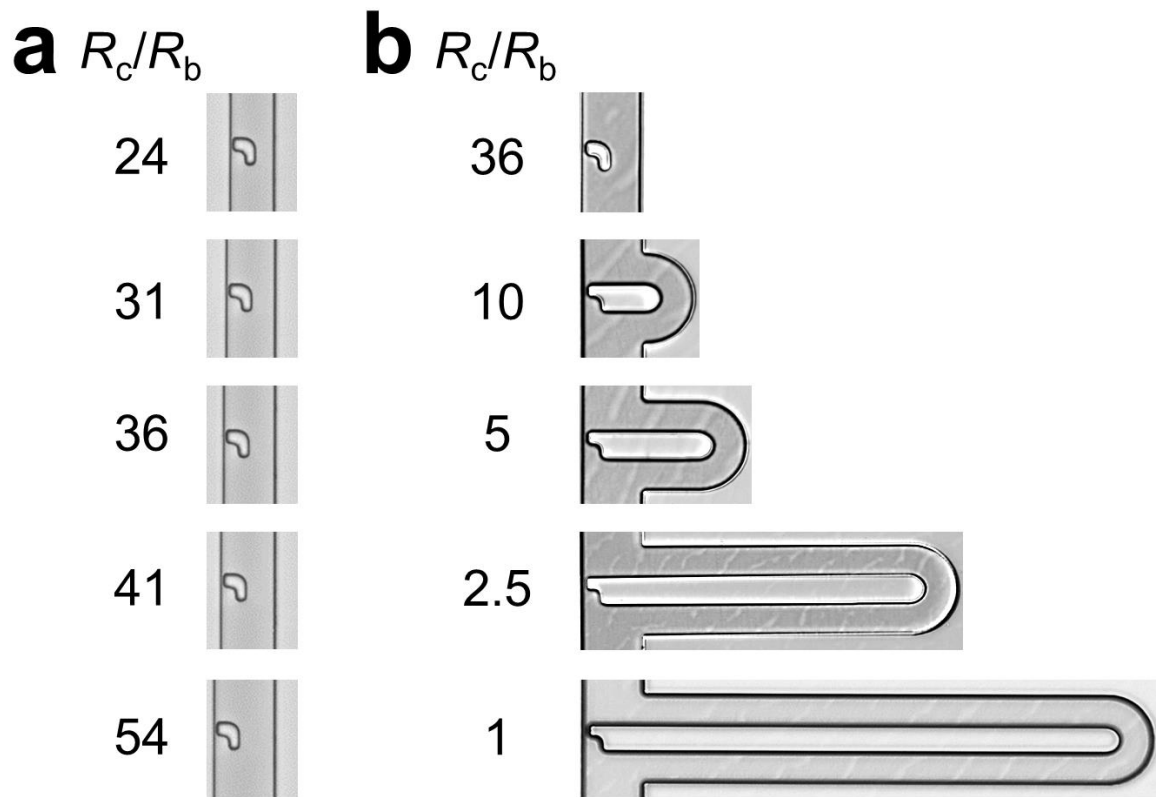


**Figure S9.** (a) Five types of hooks with increasing widths of the bypass path ( $W_b$ ). (b) Five types of hooks with increasing lengths of the bypass path ( $L_b$ ). Numbers on the left of each hook represent the corresponding fluid-resistance ratio of the capture path to the bypass path ( $R_c/R_b$ ).

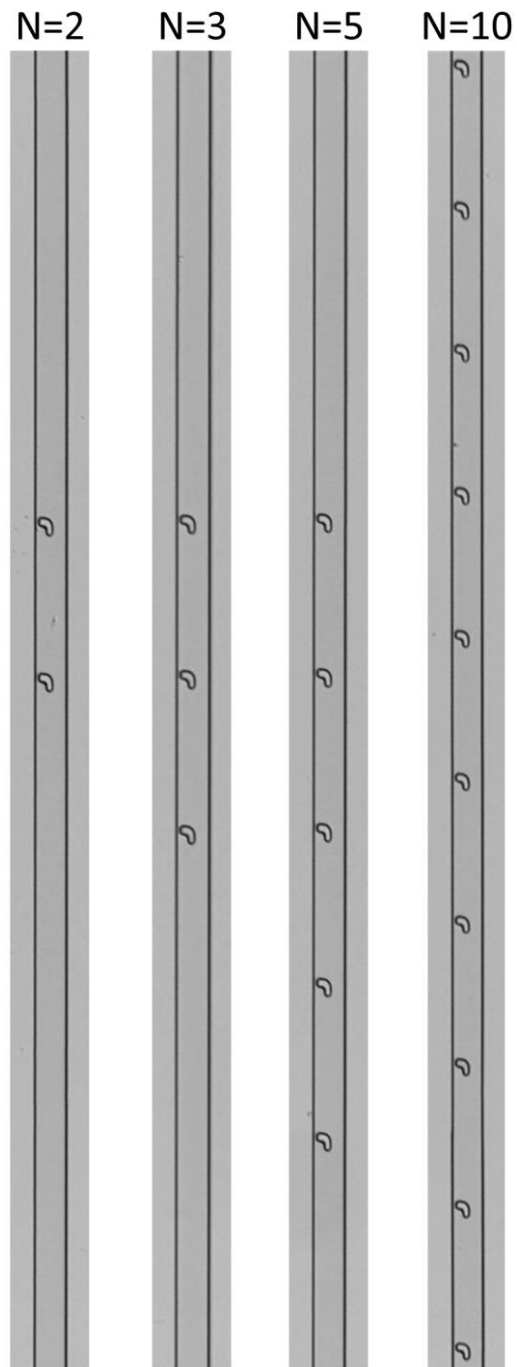


**Figure S10.** Customized hSCP tips for quantitative cell distribution. The hSCP tips containing specific numbers of hooks, including 2, 3, 5, and 10, were designed and fabricated to capture and distribute the designated number of cells into Petri dishes.

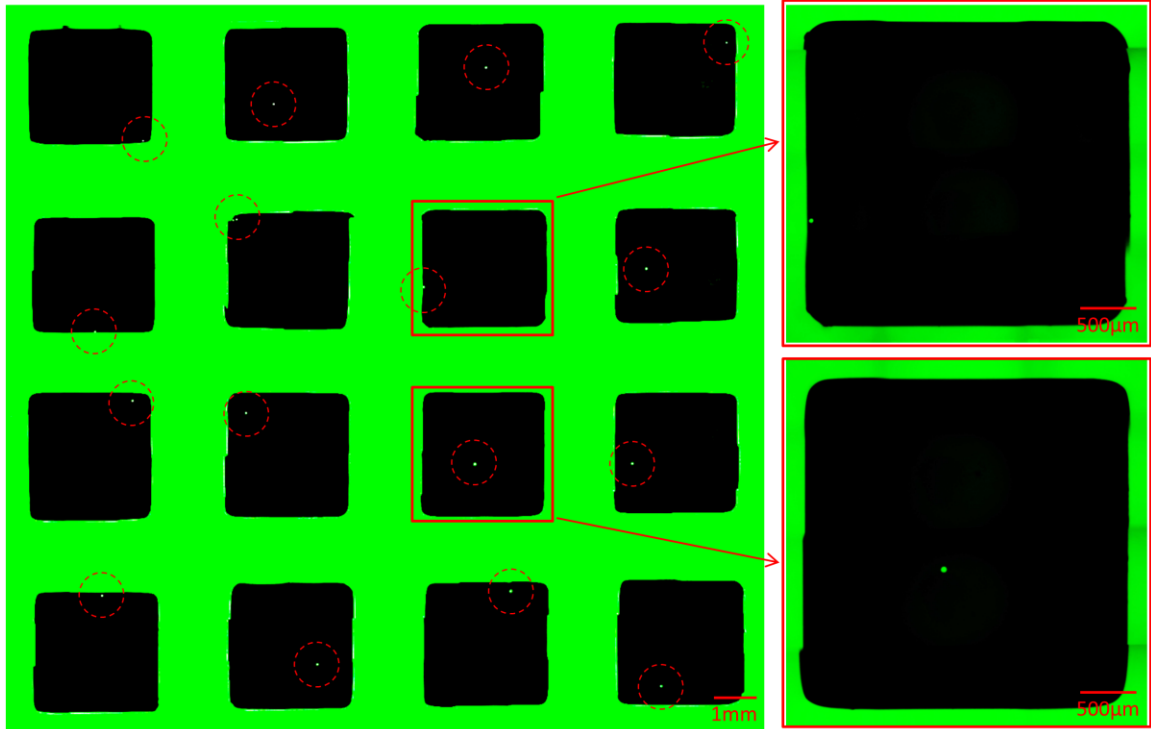


**Figure S11.** The hSCP-mediated distribution of single MDA-MB-231/GFP cells into a 4×4 array on a 384-well plate. Cells are surrounded by red dotted circles for visualization; two wells are magnified.

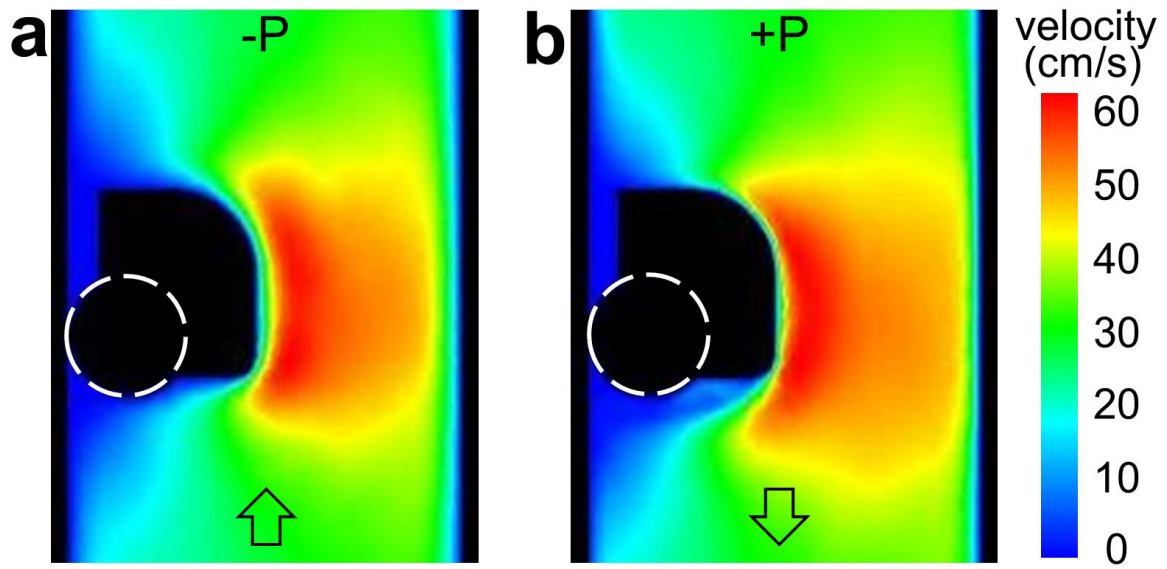


**Figure S12.** Numerical simulation of a flow profile after single-cell capture by applying  $-P$  (a) and at the moment of single-cell release by applying  $+P$  (b). The captured single cell is indicated with a white dotted circle. Black arrows represent the flow direction.

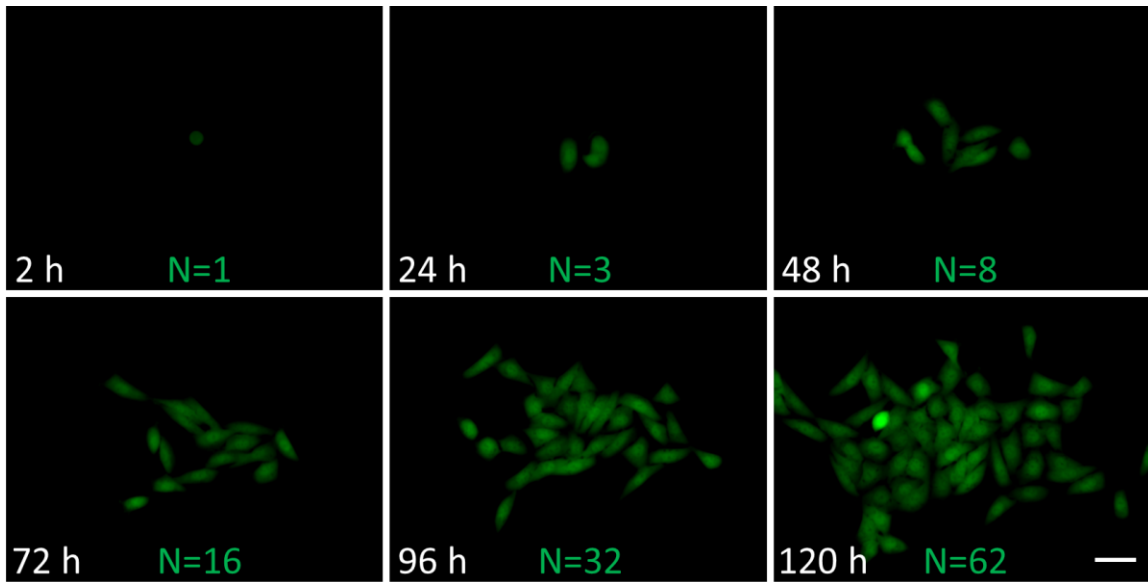


**Figure S13.** Proliferation of seeded single MDA-MB-231/GFP cells in a 96-well plate for 5 days. Hours in culture are indicated in each panel. Green numbers represent cell numbers. Scale bar=50  $\mu\text{m}$ .

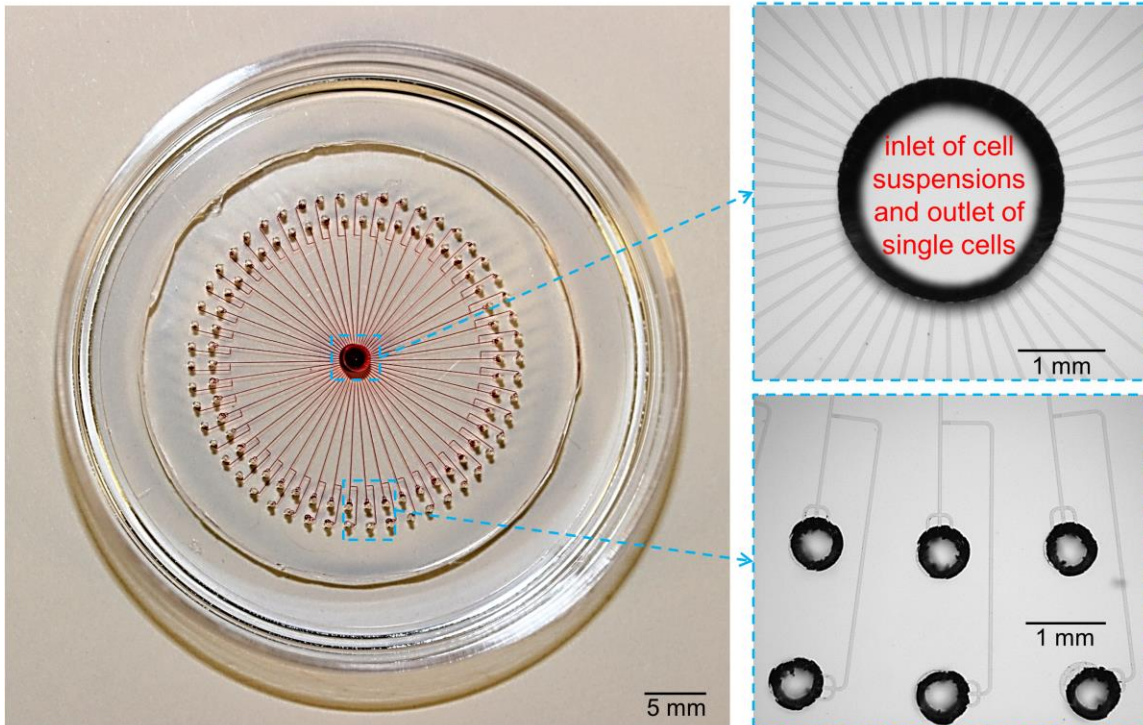


**Figure S14.** A rounded PDMS slab containing 50-plex iSCP tips was placed on a commercially available polystyrene Petri dish. Red dye was injected to aid visualization. The inlet of cell suspensions and outlet of single cells and the ports are magnified within the blue rectangles.

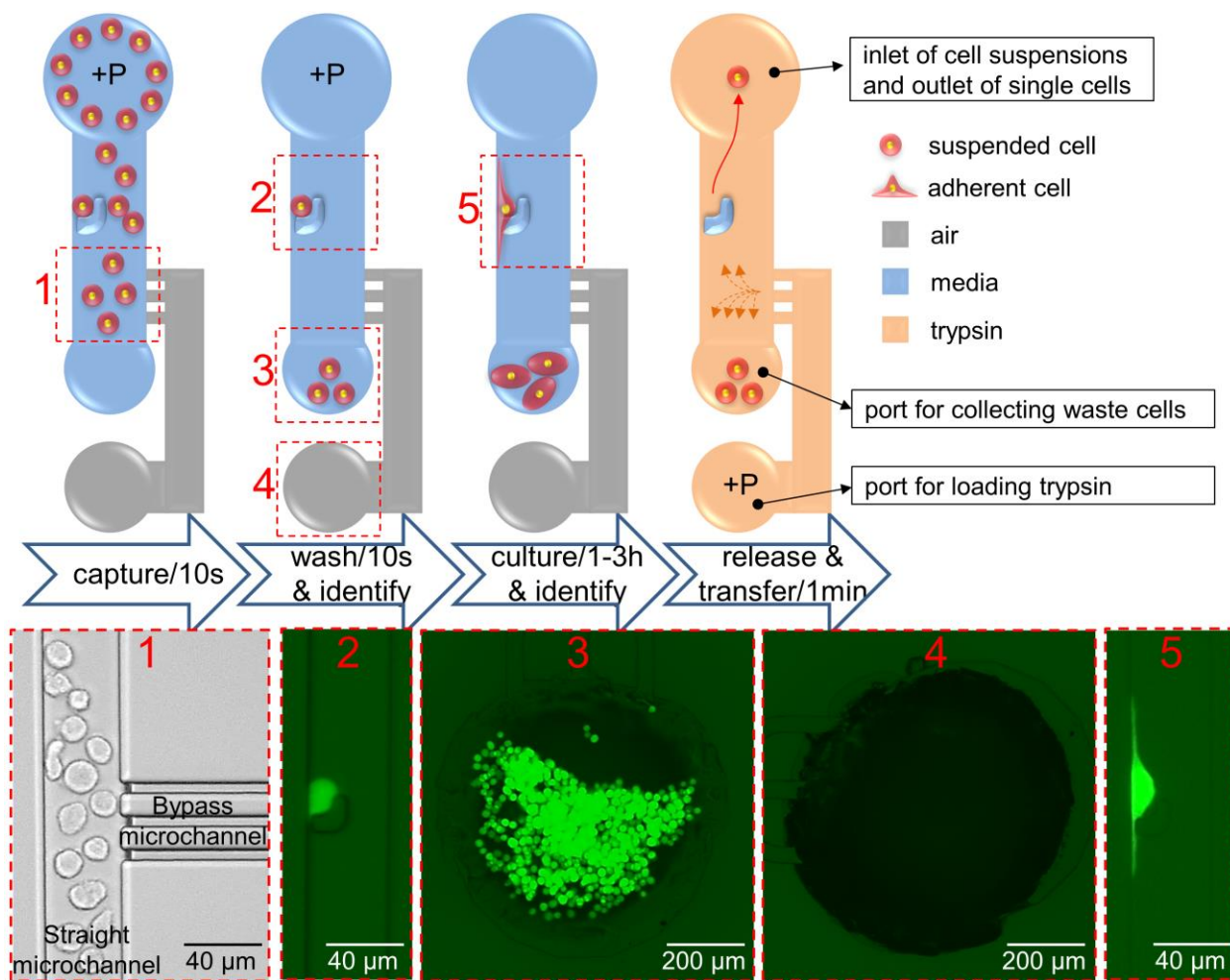


**Figure S15.** Work flow of iSCP for selective isolation of single suspended and adherent cells. (1) The bypass microchannel is trisected by a PDMS barrier to prevent cell inflow. (2) Identification of a single suspended cell by fluorescence microscopy. (3) Un-captured suspended cells are washed into the port connected to the straight microchannel. (4) No cells flow into the port connected to the bypass microchannel. (5) Identification of a single adherent cell by fluorescence microscopy. During selective isolation of single adherent cells, the desired single cells are released after capture, culture, and identification. MDA-MB-231/GFP cells were used.

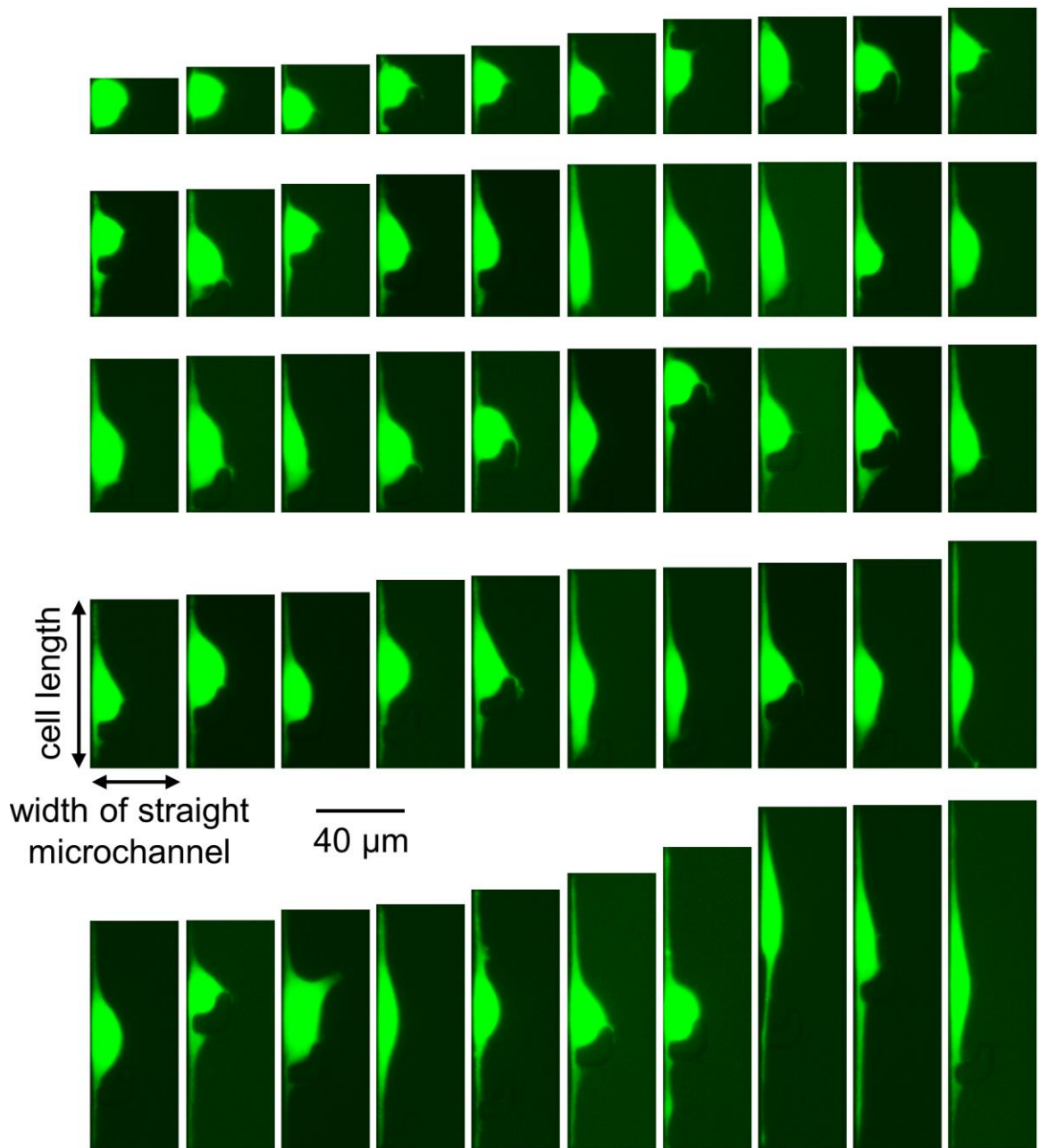


**Figure S16.** Fifty MDA-MB-231/GFP cells were imaged under a fluorescence microscope after 3 h of culture within the 50-plex iSCP-tips. Cells are ordered from the shortest cell length (upper left) to the longest cell length (lower right).

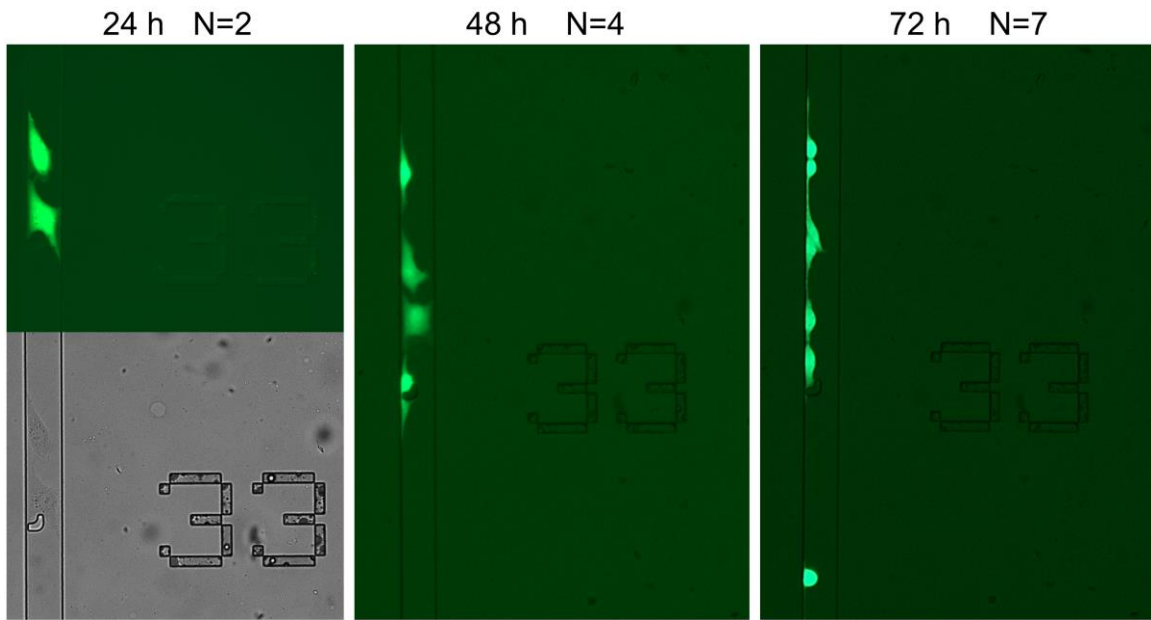


**Figure S17.** The captured single MDA-MB-231/GFP cell proliferated normally for 3 days within the 33<sup>th</sup> iSCP tip. Medium was exchanged every 12 h.

**Table S1.** Single-cell capture efficiency with various bypass path widths.

$W_b/\mu\text{m}$	15	18	20	22	27
$L_b/\mu\text{m}$	18	18	18	18	18
$D/\mu\text{m}$	12	12	12	12	12
$R_c/R_b$	24	31	36	41	54
$W_b/D$	1.25	1.5	1.67	1.83	2.25
$C/\text{no. per mL}$	$10^7$	$10^7$	$10^7$	$10^7$	$10^7$
$t/\text{s}$	5	5	5	5	5
$\alpha/^\circ$	15	30	45	60	---
$E/\%$	76.7	86.7	96.7	90	83.3

$W_b$ , width of the bypass path;  $L_b$ , length of the bypass path;  $D$ , average diameter of SK-BR-3 breast cancer cells;  $R_c$ , fluid resistance along the capture path;  $R_b$ , fluid resistance along the bypass path;  $C$ , cell number per mL;  $t$ , aspirating time;  $\alpha$ , angle between the  $x$ -axis and the line intersecting the nuclei of two cells;  $E$ , percentage of average single-cell capture efficiency

**Table S2.** Single-cell capture efficiency with various bypass path lengths.

$W_b/\mu\text{m}$	20	20	20	20	20
$L_b/\mu\text{m}$	18	65	130	260	650
$D/\mu\text{m}$	12	12	12	12	12
$R_c/R_b$	36	10	5	2.5	1
$W_b/D$	1.67	1.67	1.67	1.67	1.67
$C/\text{no. per mL}$	$10^7$	$10^7$	$10^7$	$10^7$	$10^7$
$t/\text{s}$	5	5	5	5	5
$\alpha/^\circ$	45	45	45	45	45
$E/\%$	36.7	53.3	70	86.7	96.7

$W_b$ , width of the bypass path;  $L_b$ , length of the bypass path;  $D$ , average diameter of SK-BR-3 breast cancer cells;  $R_c$ , fluid resistance along the capture path;  $R_b$ , fluid resistance along the bypass path;  $C$ , cell number per mL;  $t$ , aspirating time;  $\alpha$ , angle between the  $x$ -axis and the line intersecting the nuclei of two cells;  $E$ , percentage of average single-cell capture efficiency

**Table S3.** Comparison of methods for single-cell isolation.

Capability/ Specifics	Methods				
	Serial dilution	Micromanipulation	FACS	LCM	h/iSCP
Simplicity and time consumption	++	++	+	+	+++
Single-cell yield	+	++	+++	+	+++
Throughput	++	+	+++	+	++
Controllability in total suspension volume	+	+++	+	+	+++
Cell viability	+++	+++	+	+	+++
Cell selectivity	+	++	++	++	++
Affordability	+++	+++	+	+	+++

+++ , Excellent; ++, Intermediate; +, Poor

FACS, fluorescence-activated cell sorting; LCM, laser-capture microdissection; h/iSCP, handheld/integrated single-cell pipette

In particular, the mouth pipette is in the category of micromanipulation and seems to be very much relied on personal skills when using a researcher's mouth power to suck cells.

**Movie S1.** Handheld single-cell pipette (hSCP) for single MDA-MB-231/GFP cell isolation and identification by fluorescence microscopy.

**Movie S2.** Continuous operation of hSCP for isolation of three single MDA-MB-231/GFP cell and identification by fluorescence microscopy.

**Movie S3.** Capture and release of a single SK-BR-3 cell.

**Movie S4.** Single SK-BR-3 cells are frequently captured and then squeezed out via deformation when the fluid-resistance ratio of the capture path to the bypass path at the hook is 5.